

Chapter 6

Accelerated Testing

Abstract To perform reliability tests within a reasonable amount of time, accelerated tests are carried out in a laboratory environment in well-controlled conditions. The test condition has, therefore, to reproduce the real service conditions in an accelerated manner to achieve the same fracture mode.

Accelerated testing is conducted to determine the useful life of a certain component in the required product application. The main purpose of the accelerated test is to identify and quantify the failure and failure mechanisms that cause the component to fail.

Different accelerated tests are performed for each potential failure mechanism, as the stresses which produce failures are different for each mechanism.

There are many different failure mechanisms in microsystem products, and failures can be caused by thermomechanical, electrical, chemical, and/or environmental mechanisms.

This chapter will focus on accelerated testing of solder joints because of the prevalent use of solder in current practice. It describes both mechanical and thermal fatigue testing and the influence of different parameters on such tests, such as test frequency, stress/strain level, environmental conditions (temperature), ramp rate, and dwell time.

6.1 Fatigue Failure Analysis for Accelerated Testing

Failure mechanisms in microsystem products are many, and failures can be caused by either thermomechanical, electrical, chemical, and environmental mechanisms or a combination of the same. For a flip-chip PBGA, for example, typical failure modes can be underfill delamination, heat sink adhesive delamination, die cracking, substrate failure, PWB interconnection failure, and last but not least solder fatigue failure. The present chapter is concentrated on reliability aspects of solders and solder joints, and since thermomechanical fatigue is the main failure mechanism for solder joints, electrical, chemical, and environmental mechanisms are disregarded in the context of this chapter.

The driving force for solder joint fatigue is the thermal mismatch between the various materials in a package, resulting in significant thermal stresses/strains. Besides residual stresses generated after assembly, solder joints are particularly subjected to severe shear strains, which are the major source for solder joint fatigue.

The fatigue process begins with the accumulation of damage at a localized region or regions due to the alternating load, which eventually leads to the formation of cracks and their subsequent propagation. When one of the cracks has grown to such an extent that the remaining cross-sectional area is insufficient to carry the applied load, a sudden fracture takes place. For macroscopically isotropic materials and during fatigue, Persistent Slip Bands (PSB) are major nucleation sites for cracks. Once cracks have initiated, they grow as a result of further cyclic deformation. Fatigue crack propagation generally occurs in two stages: stage I crack growth, which takes place along slip planes or planes of maximum shear and extends only a few grain diameters from the initiation site and Stage II in which the crack follows a plane that is on an average perpendicular to the tensile axis. Due to high temperature or corrosive environments, cracks may also initiate at grain boundaries and propagate along the same [1].

Provided that a single failure mechanism is dominant, with a temperature dependent rate:

$$r = r_0 e^{-E_0/KT}, \quad (6.1)$$

where r_0 , E_0 are characteristics of the failure mechanism in question (e.g., diffusion, corrosion, etc.), the times to failure t_1 , t_2 , at temperatures T_1 , T_2 , are related by the failure rate acceleration factor:

$$\frac{t_1}{t_2} = \exp \frac{E_0}{k} \left(\frac{1}{T_1} - \frac{1}{T_2} \right), \quad (6.2)$$

and $t_1/t_2 > 1$ for $T_2 > T_1$.

6.2 Thermal Fatigue

When executing thermal fatigue testing, the sample is subjected to temperature variations, and mechanical stresses arise in the solder joints due to the dissimilar CTEs of the different materials. There are different standards stating the test conditions that should be applied. During thermal fatigue, the temperature cycles are repeated with a certain time period until fracture occurs.

In service, solders are seldom subjected to regular continuous cycles. They normally experience dwell periods of several hours or days according to performance demands. These dwell periods at constant strain levels during which stress relaxation may occur introduce an additional factor influencing life span. Furthermore, decreasing the frequency normally produces a reduction in life span for solders [2–4].

At temperatures well below one half of the absolute melting point, however, frequency has little effect on the fatigue life of most materials [3].

Due to the temperature change, the material may exhibit quite different characteristics during the run of a single thermal cycle. This makes thermal fatigue a difficult phenomenon to analyze. In particular, the location of the dwell is critical since this controls the extent of time-dependent effects.

Deformation due to thermal stresses can be classified into thermoelastic, plastic, and creep. Elastic deformation is recoverable and is caused by changes in atomic spacing. Plastic deformation is permanent and is caused by dislocation motion. Creep is a time-dependent deformation which is caused by a diffusion process. The damage in the solder joints will be, therefore, a result of thermal-activated time-dependent mechanisms (creep), cyclic mechanisms (fatigue), and microstructural changes. These damage mechanisms are expected to interact with one another and to have different relative magnitudes. They also result in detectable fatigue damage quantities, such as elastic modulus degradation, plastic strain accumulation, and microstructure phase coarsening [5]. The elastic modulus of a solder material was observed to decrease as a function of number of cycles for thermal cycling tests performed on BGA packages. The elastic modulus degradation is considered to be directly related to macromaterial degradation under fatigue, and there is a relationship between the degradation in elastic modulus and plastic strain accumulation in the material, which is related to fatigue damage evolution [6].

Thermal fatigue cannot be predicted by using the standard Coffin–Manson relationship, which only takes into account the plastic strain range [6, 7] since it can lead to inaccurate damage quantification. Both the variation in temperature, which has a significant effect on the material properties and hysteresis strain energy dissipation, and the damage mechanisms under thermal loading are quite different from isothermal mechanical loading.

Furthermore, the load-drop criterion that is normally used in isothermal low-cycle fatigue (LCF) tests and is suitable to describe macrocrack propagation, cannot accurately describe the damage evolution of solder joints under thermal fatigue. The plastic strain accumulation in the solder joints during thermal cycling is a nonlinear process and the plastic strain range of just one or several cycles cannot appropriately reflect the physical mechanism of fatigue damage evolution. A modified Coffin–Manson equation has been presented [8], which takes into account the effect of temperature:

$$N_f = CF^m(\Delta T)^{-n} \exp\left(\frac{Q}{RT_{max}}\right), \quad (6.3)$$

where N_f is the thermal fatigue life, C a constant, F the frequency, ΔT the temperature range, Q the activation energy, R the gas constant, and T_{max} the maximum temperature.

To predict thermal fatigue behavior of solder joints, it is more accurate, however, to use the hysteresis energy-based damage which takes into account both strain and stress [7].

6.3 Effect of Different Test Factors on Thermal Fatigue Life

Thermal fatigue life is dependent on many different factors. It depends among other factors on the maximum (T_{max}) and minimum (T_{min}) temperature applied and the temperature range used ΔT . The larger the temperature differences, the higher the damage per cycle [9]. In general, the larger the maximum temperature T_{max} , temperature range ΔT , and dwell time and the faster the ramp rate, and the higher the stress level applied, the shorter the fatigue life [10]. The effect of heating rate on damage accumulation of Sn–Ag solder joints was investigated and found that a faster heating rate was more damaging compared with slower heating rate. The same results were obtained by Qi et al. [9]. Regarding hold time, increasing the hold time will decrease the fatigue life as a result of time-dependent creep.

Fatigue life definition has also an effect on thermal fatigue life. The Coffin–Manson cyclic strain-hardening exponent, α , was found to decrease when increasing the stress range drop parameter, Φ [$\Phi = 1 - (\Delta\tau/\Delta\tau_{max})$]. It changed from 0.74 to 0.49 when changing the failure criterion from 10 to 50%. This variation of k as a function of failure definition reflects the difference in the rates of stress-range drop at different stages of cycling [11].

A summary of the effect of different factors on the thermal fatigue life of solder joints is shown in Table 6.1.

As pointed out before, creep is a phenomenon that also contributes to solder joint failure. The higher the temperature, the higher the contribution of creep. Creep strain is a result of thermally activated, time-dependent mechanisms. These mechanisms can obey a constitutive relation, as in (6.4):

$$\dot{\epsilon} = C \left(\frac{1}{d}\right)^a \frac{1}{kT} \left(\frac{\sigma - \sigma_b}{E(T)}\right)^n \exp\left(-\frac{Q}{kT}\right), \tag{6.4}$$

Table 6.1 Effect of some factors on the thermal fatigue life of solder joints

Factor	Factor changes	Fatigue life changes	Comments
Frequency	Decrease	Decrease	At temperatures well below one half of the absolute melting point, frequency has little effect on the fatigue life of most materials
Hold time	Increase	Decrease	Hold time is much more destructive than ramp time (much lower strain rates operating during hold time)
T_{max}	Higher	Decrease	–
ΔT	Higher	Decrease	–
Heating/cooling rate(ramp rate)	Faster	Decrease	–
Failure definition	Decrease	Decrease	Higher strain hardening exponent α , at earlier stages of testing

where C is a constant, d refers to the grain size, a to the grain size sensitivity, σ is the applied stress with σ_b being the back stress, $E(T)$ the modulus as a function of temperature, and n is the stress exponent. The thermal activation of creep is characterized by an activation energy Q and k is the Boltzmann's constant. At high stresses, creep is controlled by dislocation movement. When dislocation entanglement and recovery reaches an impasse, where the rate of hardening is equal to the rate of recovery, a quasi-steady state is reached that obeys (6.4). This creep rate is then controlled by the rate at which edge dislocations can climb out of their slip planes. At lower stresses, creep is controlled by the motion of vacancies, from grain boundary to grain boundary. At the highest temperatures, vacancy motion happens by lattice diffusion and the creep is referred as Nabarro–Herring creep. At lower temperatures, vacancy motion happens through grain boundary diffusion and the creep mechanism is referred to as Coble creep. The damage that is stored during creep deformation can be of three types: creep cracks, void nucleation and growth, and microstructural degradation. Microstructural degradation is often the most serious damage in alloys that depend on the phase morphology for creep resistance. Stresses at high temperatures allow strengthening precipitates to coarsen and change shape, weakening the alloy.

For the steady state, creep follows the Garofalo–Arrhenius equation, expressed as:

$$\dot{\gamma} = C \left(\frac{G}{T} \right) \left[\sinh \left(\omega \frac{\tau}{G} \right) \right]^n \exp \left(-\frac{Q}{kT} \right), \quad (6.5)$$

where $\dot{\gamma}$ is the steady-state creep shear strain rate, t the time, C a material constant, G the temperature-dependent shear modulus, T the absolute temperature (K), ω defines the stress level at which the power law stress dependent breaks down, τ the shear stress, n the stress exponent, Q the activation energy for a specific diffusion mechanism (dislocation diffusion, solute diffusion, lattice self-diffusion, and grain boundary diffusion), and k the Boltzmann's constant (8.617×10^{-5} eV/K).

6.4 Isothermal Mechanical LCF

During isothermal mechanical fatigue testing, samples are cycled mechanically with a constant stress or strain amplitude, at a constant temperature. The testing executed with constant strain amplitude and where plastic strains are dominant is also called LCF.

A commonly used method to characterize LCF behavior of solder joints is the load/stress versus number of cycles. The pattern of load/stress reduction as a function of number of cycles can be described by a so-called load-drop parameter, defined in (6.6) as:

$$\Phi = 1 - \frac{\Delta F}{\Delta F_M}, \quad (6.6)$$

where ΔF is the load range at a certain load cycle number and ΔF_M is the maximum load range over the initial few cycles. The load-drop parameter curves can be divided into three different stages: the first called the rapid increase stage, the second the steady stage, and the third the acceleration stage. The steady stage is generally the dominating stage of the fatigue life and hence the slope of the load-drop parameter curve in the steady stage reflects the LCF life; the flatter the slope of the steady stage, the longer the fatigue life.

It is normally important to investigate, if the fatigue life is related to the applied plastic strain. The Coffin–Manson fatigue model is often used for the LCF analysis of solders. The Coffin–Manson relationship assumes that LCF failure is strictly a result of plastic deformation and the elastic strain has a negligible effect on the LCF life. The elastic strain range can also be included in the calculation, and the fatigue life is then defined in terms of both plastic and elastic strains. The relationship is given by:

$$\gamma_t = \gamma_e + \gamma_p = \left(\frac{N_f}{C_B}\right)^{-1/\alpha} + \left(\frac{N_f}{C_{CM}}\right)^{-1/\alpha}, \quad (6.7)$$

In principle, both equations could be used to define fatigue life, N_f , for a given strain. For LCF applications, however, it is the correlation with the plastic strain that is used to predict fatigue life and since the elastic strain is generally very small in comparison to the plastic strain, which is the factor that really causes fatigue, this is normally ignored.

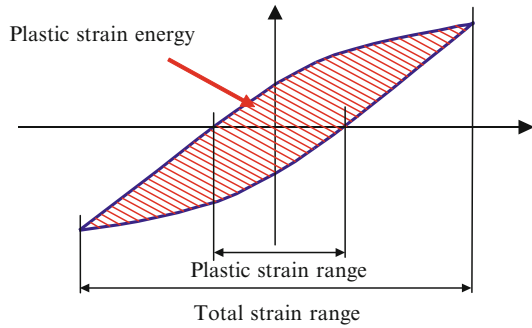
There is of course a third factor that is also important in the context of solder joint fatigue failure and that is creep. For solders, the cyclic creep effects are more pronounced at higher temperatures and slower test frequencies, decreasing the fatigue lives. Hence, the constants on the Coffin–Manson relationship are dependent on both test temperature and cyclic frequency. One disadvantage with the Coffin–Manson relation is that it only accounts for strain and not stress. For those reasons, another model that is increasingly being applied in the prediction of fatigue life of solder joints is the Morrow's energy density model. This model predicts fatigue life in terms of plastic strain energy density (W_p), and takes therefore into account both strain and stress:

$$N_f^m W_p = C, \quad (6.8)$$

where m is the fatigue exponent and C is the material ductility coefficient. The strain energy density is measured as the area of the hysteresis loops. The fatigue exponent and the material ductility coefficient are also dependent on test frequency and temperature.

The stress–strain history consists of the so-called hysteresis loops. The area of the hysteresis loop represents the energy dissipated in the material within one cycle. In the course of cyclic loading, materials can either harden or soften depending on their prior thermomechanical treatment. The primary hardening or softening period, which occurs quite rapidly in the early portion of fatigue life, is usually

Fig. 6.1 Stress–strain hysteresis loop



followed by a steady-state cyclic deformation in which the stress–strain response remains constant. The hysteresis loop for a constant cyclic loading can be observed in Fig. 6.1.

The hysteresis loops provide very useful information for engineering evaluations of solder joint reliability. The width of the loop gives an estimate of the plastic strain range (intersection between the loop and the strain axis at zero stress). The total strain $\Delta\varepsilon$ is the sum of both the elastic and plastic strains.

6.4.1 Effect of Frequency

The effect of frequency on the isothermal mechanical fatigue life of most metals is dependent on the test temperature. For temperatures well below half of the absolute melting temperature, frequency has little effect on the fatigue life of most metals. Over this value, however, a reduction in frequency results in a decrease in fatigue life (N_f) for many metals, including solders. The reason for this behavior is that at high temperatures, creep failure, which is time dependent, plays a very important role in damage accumulation. Isothermal LCF tests performed on flip-chip solder joints showed that longer wave periods (slower frequency) leads to higher crack growth rates than shorter wave periods (higher frequency).

Some alloys, however, show frequency transition regimes, under or above which changes in frequency do not result in any appreciable fatigue life changes. For the Pb–3.5Sn, for example, the number of cycles to failure decreased steadily when cycling frequency was reduced below 10^{-2} Hz; however, no effect of frequency on N_f was detected at frequencies higher than 10^{-2} Hz. For this Pb-rich alloy, the effect of frequency was also found to be a function of strain range. The fatigue life of eutectic Sn–37Pb was also found to be frequency dependent over the test frequency range of 10^{-4} to 1 Hz. The decrease in fatigue life, however, was small when frequency decreased from 1 to 10^{-3} Hz, but became larger when the frequency was reduced further from 10^{-3} to 10^{-4} Hz. For the lead-free Sn–3.5Ag solder, the fatigue life also decreased as the frequency decreased from 1 to 10^{-3} Hz.

For other LCF tests performed with Sn–0.7Cu, increasing the frequency from 10^{-3} to 1 Hz significantly reduced the stress range and the plastic strain energy density. The fatigue life, tested at total strain ranges of 2.5 and 7.5%, at 398 K decreased linearly with decreasing frequency from 1 to 0.01 Hz.

The reduction in fatigue life with decreasing test frequency is attributed to the increasing exposure to creep and stress relaxation effects during fatigue testing. As the frequency decreases, the time for completing one cycle increases, which allows for longer exposure for creep and stress relaxation to develop and leads to a reduction in the stress range and hysteresis inelastic energy density.

To take into account the frequency during isothermal LCF tests, a frequency modified Coffin–Manson relationship can be used, which states:

$$\left[N_f v^{(k-1)} \right]^m \Delta \gamma_p = C, \quad (6.9)$$

where v is the frequency and k is the frequency exponent. Both ramp and hold time effects are considered because frequency is the inverse of the period, which is the sum of the ramp times and the hold times. The effect of frequency is determined by the magnitude of k . For $k = 1$, there is no dependence of the fatigue life with frequency variations and the frequency term is equal to 1 (for very low life, $N_f < 50$). When $k = 0$, the fatigue life is modified by $1/v$, and if the frequency is halved, the number of cycles to failure is also halved, which results in a constant time to failure [N/v is the time to failure which results in the development of a constant time to failure (for a given applied plastic strain range)]. When the plastic strain range is constant, the fatigue life shows a linear relationship with frequency in a log–log plot, and where the slope of the curve is the value of $(1-v)$.

The frequency-modified Morrow model is the following:

$$\left[N_f v^{(h-1)} \right]^n W_p = A, \quad (6.10)$$

where v is the frequency and h is the frequency exponent. The frequency exponent k can be determined from the relationship between fatigue life and frequency. For a constant strain range, this relationship can be expressed as:

$$N_f = b v^{1-k}, \quad (6.11)$$

where b is a constant and k is the frequency exponent.

6.4.2 Effect of Dwell (Hold) Time

In general, increasing the dwell time will decrease the fatigue life of solders. This is also a result of longer exposure to creep and stress relaxation. For lead-rich alloys, tested at room temperature and under a strain-controlled LCF, the dwell time was

found to have a very high effect on fatigue life compared with other factors such as ramp rate, and increasing the dwell time decreased the fatigue life. Tensile hold times are more damaging compared with compressive hold times during high temperature fatigue of solders, and the fatigue life decreases when the tensile hold time is increased.

6.4.3 Effect of Strain Range and Strain Rate

Increasing the strain amplitude (strain range) results in a decrease in fatigue life [12]. The fatigue life of eutectic Sn–37Pb bulk alloy was found to decrease with increasing total strain range at a given temperature and frequency.

The effect of strain rate on the isothermal LCF of bulk Sn–37Pb was studied and the results showed a decrease in fatigue life with decreasing strain rate. They found, however, a transition regime at some intermediate strain rate and this relationship showed a typical S-shaped characteristic. The effect of strain rate on fatigue life became smaller with increased total strain range. The reason for this was found to be different failure mechanisms, where cavitation due to grain boundary sliding was the dominant failure mechanism in the low strain rate regime, while cavitation without grain boundary sliding was the dominant failure mechanism in the high strain rate regime. The transition strain rate was found to be $\sim 10^{-3}$ – 10^{-4} per second.

6.4.4 Effect of Temperature

In general, for all metals, an increase in temperature results in a decrease in isothermal fatigue life. The degree of fatigue life change depends, however, on the material and testing conditions. Above $0.6 T/T_m$, the contribution of creep is expected to increase with increased temperature, which will result in shorter fatigue life. As the temperature increases the plastic strain range increases and the stress range decreases. It has been found, however, for a Pb-rich alloy, that the fatigue life dependency on temperature only follows approximately an Arrhenius equation between 25 and 80°C.

The eutectic Sn–37Pb alloy, tested as bulk material, was found to be temperature dependent over the range of test temperatures (–40 to 150°C). As the temperature increased, the fatigue life decreased linearly on a log–log plot.

6.4.5 Effect of Failure Definition

For isothermal LCF tests, changing the definition of failure will also affect the fatigue life. For LCF tests performed at room temperature, the fatigue life decreases

as the load-drop failure definition decreases from 70 to 20% load drop. This conclusion is rather obvious; however, when comparing, and for that matter using, fatigue life data from different researchers, it is very important to know which failure definition was used since in addition to a decrease in fatigue life when decreasing the load-drop parameter, the slope of the plastic strain versus fatigue life plot will also change.

6.4.6 Effect of Other Factors

Many of the new lead-free solder alloys perform better in fatigue compared with the eutectic Sn–37Pb. Isothermal LCF tests performed at room temperature and at different loading angles showed that the fatigue life of Sn–3.5Ag–0.75Cu was longer for all loading conditions compared with the Sn–37Pb alloy.

The fatigue behavior of a solder alloy is affected by the addition of other elements. Under LCF tests of lap-shear samples, at room temperature and 0.1 Hz, the fatigue life of Sn–3.5Ag– x Sb increases when increasing the amount of Sb from 1.73 to 10.05 wt% [13].

A summary of some factors and their effects on isothermal LCF life is depicted in Table 6.2.

The effect of creep on the fatigue life of the solder joints tested under isothermal LCF conditions (at room temperature) was not taken into consideration in the present work. By using relatively large strain range amplitudes, triangular wave shapes without any hold time and a relatively high frequency of 0.2 Hz decreases the effect of creep. For isothermal LCF tests performed at room temperature (25°C), the effect of creep can be disregarded when the testing frequency is higher than 10^{-3} Hz. It is known, however, that fatigue life is also dependent on test temperature, and the higher the temperature, the lower the fatigue life, which is a result of time-dependent creep.

Table 6.2 Overall effect of different factors on isothermal low cycle fatigue life

Factor	Factor changes	Fatigue life changes	Comments
Frequency	Decrease	Decrease	Dependent on test temperature: at $T < \frac{1}{2} T_m$, frequency has little effect on fatigue life
Hold time	Increase	Decrease	Tensile hold time is more detrimental compared with compressive hold time. Hold time is more detrimental than ramp time
Strain range	Increase	Decrease	At a given temperature and frequency
Strain rate	Decrease	Decrease	–
Temperature	Increase	Decrease	–
Failure criteria	Decrease	Decrease	The slope of the plastic strain versus fatigue life plot will also change

Exercises

6.1 A FCOB assembly with a solder-bumped height of 0.1 mm and a distance from the neutral point of 0.3 mm is subjected to a cyclic temperature from -55 to $+125^\circ\text{C}$. The coefficients of thermal expansion for silicon and FR-4 are 2.3 and 18 ppm/ $^\circ\text{C}$, respectively. For the simple case without underfill encapsulant, calculate the solder joint strain range, $\Delta\gamma$, and the fatigue life prediction model, N_f , as given by Engelmaier's model in question 4. If an underfill encapsulant is applied on the flip-chip assembly, discuss how the solder joint shear strain range can be estimated? Is finite-Element Analysis necessary? How does the estimated fatigue life compare with the case without encapsulant. The following parameters are given:

- $h = 0.1$ mm
- DNP = 3 mm
- $\Delta T = -55 + 125 = 180^\circ\text{C}$
- $\text{CTE}_{\text{silicon}} = 2.3$ ppm/ $^\circ\text{C}$
- $\text{CTE}_{\text{FR-4}} = 18$ ppm/ $^\circ\text{C}$.

6.2 The homologous temperature for one metal is a ratio between the temperature involved and its melting point. That is

$$T_h = \frac{T}{T_{\text{melt}}},$$

where the temperature is expressed in degrees absolute.

At homologous temperatures greater than 0.5, metals exhibit significant stress relaxation and creep. To describe the steady-state creep shear strain, Darveaux gave us the relationship as:

$$\begin{aligned} f(\tau) &= C \left[\sinh \left(\omega \frac{\tau}{G} \right) \right]^n \\ g(t) &= t \\ h(T) &= \left(\frac{G}{T} \right) \exp \left(\frac{-Q}{kT} \right), \end{aligned}$$

where τ is the shear stress, G the shear modulus, ω defines the stress level at which the power law stress dependence breaks down, k the Boltzmann constant, Q the activation energy, n the stress exponent, C a constant, and T the absolute temperature.

Calculate the homologous temperature for eutectic solder at room temperature (its melting point is 180°C). What is the Darveaux's constitutive law for eutectic solder? What is the steady-state creep shear strain rate?

6.3 Figure 6.2 below shows a CSP assembly. The chip was attached to the ceramic interposer (substrate) with gold bumps and underfill epoxy, and then soldered to the PCB. The chip size was $7 \times 7 \times 0.41$ mm with 100 peripherally distributed gold bumps on a 0.25-mm pitch. The heights of the gold bumps were 0.025 mm as shown in Fig. 6.3 (not drawn to scale, and we only draw 20 instead of 100 gold bumps on the chip). The ceramic interposer dimensions were $7.45 \times 7.45 \times 0.25$ mm. There were 100 arrayed eutectic solder bumps at the bottom of the ceramic substrate as shown in Fig. 6.4 (not drawn to scale, and we only draw 16 instead of 100 solder bumps on the ceramic substrate).

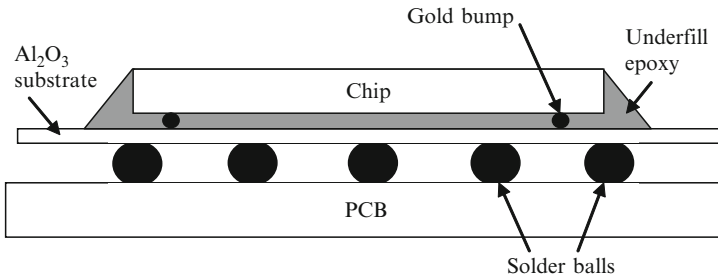


Fig. 6.2 Schematic cross section of a chip-scale package (CSP) assembly

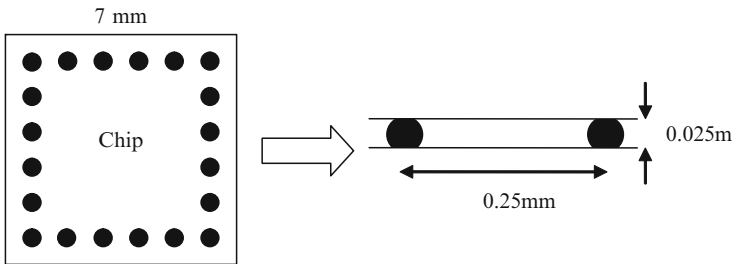


Fig. 6.3 Chip size and gold bump pitch for the CPS (not drawn to scale)

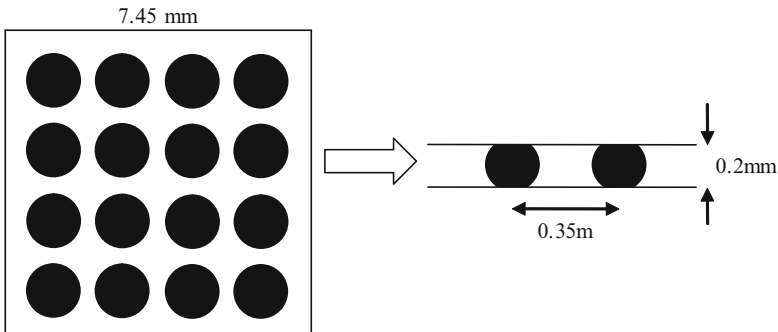


Fig. 6.4 Ceramic substrate and the eutectic solder balls on PCB (not drawn to scale)

After the CSP was assembled on the PCB, the solder ball height was about 0.2 mm.

A temperature loading is imposed on the CSP assembly from -40 to 125°C with 10-min ramp and 20-min hold. The CTE mismatch between the chip, ceramic substrate, and the PCB brought the damage of the device (the typical CTE values are $\alpha_{\text{chip}} = 5 \text{ ppm/K}$, $\alpha_{\text{ceramic}} = 10 \text{ ppm/K}$, and $\alpha_{\text{PCB}} = 16 \text{ ppm/K}$).

Question 1: What is the shear strain imposed on the gold bumps when it has no underfill?

Question 2: Consider the eutectic solder bump which is the farthest away from the chip center (assuming the distance equals half of the ceramic substrate edge), what is the shear strain on it?

Question 3: Assuming both gold bumps and eutectic bumps in this study are obeyed the same Coffin–Manson equation with the exponential number -2 , the lifetime for solder bumps is what times more than that of gold bumps? (this situation has been changed because of the existence of underfill)

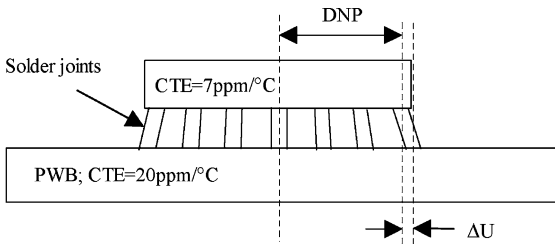
Question 4: An interesting phenomenon is observed in experiments. For the eutectic bumps on PCB, the farther distance from the chip center, the easier they will be damaged. Can you explain it?

Given:

Chip size: $7 \times 7 \times 0.41 \text{ mm}$ with 100 gold bumps on a 0.25-mm pitch Height of the gold

Bumps: 0.025 mm

Ceramic substrate: $7.45 \times 7.45 \times 0.25 \text{ mm}$, 100 solder bumps (0.2 mm high after reflow)



DNP (distance to neutral point)= $L=11.4 \text{ mm}$

Temperature cycle: -40 to 125°C with 10-min ramp and 20-min hold.

6.4 Ceramic ball grid array (CBGA) package.

Thermal cycling \Rightarrow different expansion of the different parts \Rightarrow the relative displacement ΔU of a solder joint is calculated from the difference between the top and the bottom surfaces of the solder joint.

When the temperature raises by 100°C , what is the relative displacement in the right end solder joint? Estimate the maximum shear strain range ($\Delta\gamma$) in the

Table 6.3 Life time and mean plastic shear strain range for type A and type B

	Type A	Type B
N_f	87	2,250
$\Delta\gamma$	0.0866	0.0101

solder joint of a perimeter PBGA package assembled onto an FR-4 PWB subjected to a temperature range of 0–100°C. The package has a DNP = 17 mm to the outermost solder joint and the solder height is 0.5 mm. The CTE of the BT (Bismaleimide Triazine) substrate is 15 ppm/°C and for the FR-4 PCB the CTE is 18 ppm/°C. The effective CTE of the mold compound and silicon die may be assumed to be the same as the BT substrate.

- 6.5 The solder joint fatigue life for the perimeter PBGA given in question 3 can be assessed using Engelmaier’s Model for solder joint fatigue prediction. Two thermal cycling profiles are to be evaluated. The first temperature profile is from +25 to +125°C with a cycle time of 40 min. The second temperature profile is from –20 to +80°C with a cycle time of 24 min. Which temperature profile is more damaging in fatigue life?
- 6.6 The Coffin–Manson relation is based on that the solder joint failure is dependent on the accumulation of the plastic strain damage. It has been widely used to predict the thermal fatigue life of solder joints.

$$N_f = C(\Delta\gamma)^\beta,$$

where N_f is the number of the cycles of failure, $\Delta\gamma$ is the plastic shear strain range, C and β are the material constants. There are two types of flip-chip electronic package (type A and type B) with the same material while different geometry. Table 6.3 gives the lifetime N_f measured by accelerated test and the plastic shear strain range $\Delta\gamma$ calculated by FEM simulation.

Please calculate the empirical parameters C and β in the Coffin–Manson equation for this kind of flip-chip package using the data from Table 6.3.

References

1. F. Ellyin (Ed.), “Fatigue damage crack growth and life prediction”, Chapman & Hall, London, 1997.
2. H. D. Solomon, “Fatigue of 60/40 solder”, IEEE Transactions on Components, Hybrids and Manufacturing Technology, CHMT-9(4), 1986, 423–432.
3. S. Vaynman, “Fatigue life prediction of solder material: Effect of ramp time, hold time and temperature”, Proceedings of the 40th Electronic Components and Technology Conference, 1, 1990, 505–509.
4. X. Q. Shi, H. L. J. Pang, W. Zhou, Z. P. Wang, “Low cycle fatigue analysis of temperature and frequency effects in eutectic solder alloy”, International Journal of Fatigue, 22, 2000, 217–228.

5. C. Basaran, H. Tang, S. Nie, "Experimental damage mechanics of microelectronic solder joints under fatigue loading", *Electronic Components and Technology Conference*, 1, 2005, 874–881.
6. H. Tang, C. Basaran, "Experimental characterization of material degradation under fatigue loading", *IEEE, The Eighth Intersociety Conference on Thermal and Thermomechanical Phenomena in Electronics, IThERM*, 2002, 896–902.
7. V. Sarihan, "Energy based methodology for damage and life prediction of solder joints under thermal cycling", *IEEE Transactions on Components, Packaging and Manufacturing Technology-Part B*, 17(4), 1994, 626–631.
8. I. Shohji, H. Mori, Y. Orii, "Solder joint reliability evaluation of chip scale package using a modified Coffin-Manson equation", *Microelectronics Reliability*, 44, 2004, 269–274.
9. Y. Qi, R. Lam, H. R. Ghorbani, P. Snugovsky, J. K. Spelt, "Temperature profile effects in accelerated thermal cycling of SnPb and Pb-free solder joints", *Microelectronics Reliability*, 46, 2006, 574–588.
10. H. Cui, "Accelerated temperature cycle test and Coffin-Manson model for electronic packaging", *IEEE RAMS*, 2005, 556–560.
11. X. W. Liu, W. J. Plumbridge, "Thermomechanical fatigue of Sn-37 wt% Pb model solder joints", *Materials Science and Engineering A*, 362, 2003, 309–321.
12. S. Vaynman, M. E. Fine, "Effects of strain range, ramp time, hold time and temperature on isothermal fatigue life of tin-lead solder alloys", in *Solder joint reliability – theory and applications*, edited by J. H. Lau, Van Nostrand Reinhold, New York, 1991.
13. H. T. Lee, H. S. Lin, C. S. Lee, P. W. Chen, "Reliability of Sn-Ag-Sb lead-free solder alloys", *Materials Science and Engineering A*, 407, 2005, 36–44.